TORSION OF A CIRCULAR SHAFT WITH DIAMETRICALLY OPPOSITE FLAT SIDES

DONALD H. REESE

Artisan Gold Lettering & Smith Bindery

593 - 15th Street Oakland, Calif. GLencourt 1-9827

DIRECTIONS FOR BINDING

BIND IN
(CIRCLE ONE)

BUCKRAM 8854
COLOR NO._____

FABRIKOID
COLOR_____

LEATHER
COLOR_____

OTHER INSTRUCTIONS

LETTERING ON BACK shelf
TO BE EXACTLY AS
PRINTED HERE.

REESE

1954

Thesis
R275

Letter on the front cover:

TORSION OF A CIRCULAR SHAFT WITH
DIAMETRICALLY OPPOSITE FLAT SIDES

DONALD H. REESE

TORSION OF A CIRCULAR SHAFT WITH DIAMETRICALLY OPPOSITE FLAT SIDES

Donald H. Reese

TORSION OF A CIRCULAR SHAFT WITH DIAMETRICALLY OPPOSITE FLAT SIDES

by

Donald H. Reese

Lieutenant, U. S. Navy

Submitted in partial fulfillment

of the requirements

for the degree of

MASTER OF SCIENCE

in

MECHANICAL ENGINEERING

United States Naval Postgraduate School

Monterey, California

1954

This work is accepted as fulfilling

the thesis requirements for the degree of

MASTER OF SCIENCE

in

MECHANICAL ENGINEERING

from the

United States Naval Postgraduate School

PREFACE

The research reported here was done at the U. S. Naval Postgraduate School, Monterey, California during the period February through April, 1954. The work was undertaken to determine experimentally the maximum stress and the torsional rigidity of a round shaft with diametrically opposite parallel flat sides. This information was obtained for several configurations by direct experiment and for one configuration by an electrical analogy.

The author is greatly indebted to Prof. R. E. Newton for many helpful suggestions and much constructive criticism and assistance in the preparation of this manuscript. In addition the author wishes to thank Mr. Norman Walker for the extreme care and patience exercised in the preparation of the test specimens. It is further desired to acknowledge the help of F. N. Lauck, Ph3, USN, who did the photographic work which appears in the thesis.

TABLE OF CONTENTS

CHAPTER	TITLE	PAGE
	Preface	ii
	List of Illustrations	v
	Index of Symbols	vi
	Summary	1
I	An Introduction to the Problem	
	1. Statement of the problem	2
	2. State of stress for a solid round shaft with diametrically opposite parallel flats.	2
	3. Previous solutions to the problem	2
	4. Electrical Analogy	3
II	Material and Testing Technique Employed	
	5. Specimen material and dimensions	8
	6. Method of machining specimens	8
	7. Strain gage selection and application	10
	8. Angle of twist measurement	13
	9. Strain gage tests	14
	10. Analog experiment	14
III	Reduction of Data	
	11. Strain gage calibration	20
	12. Electrical Analogy	21
IV	Results and Discussion	
	13. The Results	24
	14. Comparison with previous solutions	25
	15. Sources of error	27

TABLE OF CONTENTS

CHAPTER	TITLE	PAGE
V	Conclusion	28
	Bibliography	29

LIST OF ILLUSTRATIONS

FIGURE	TITLE	PAGE
1	Cross Section of the Shaft	2
2	Bar in Torsion	3
3	Cross Section of the Shaft	4
4	Analog Experimental Assembly	6
5	Specimen Details	9
6	Strain vs. Torque for A-19 Strain Gage	12
7	Schematic Diagram for Optical System used for Angle of Twist Measurement	13
8	Experimental Equipment Set Up	15
9	Potential Distribution Along the Boundary x=w	18
10	Equipotential Traces of Electrical Analog	22
11	Experimental Potential vs. Distance Along x-axis	23
12	Comparison with Previous Investigations	26

TABLE NO.	TITLE	PAGE
1	Specimen Dimensions	8
2	A-19 Strain Gage Results	11
3	Potentials Maintained Along Boundary	14
4	Values of Maximum Shear Stress and Twisting Moment	24

INDEX OF SYMBOLS

ϕ Stress Function

z, x, y Coordinates

G Shear modulus for the material

θ Angle of twist in radians per unit length

τ Shearing stress

M_t Torsional moment

K Constant of proportionality

ϵ Strain

e Apparent strain

V Potential

P Experimental potential

p Angle of twist

Δh Change in distance between 2 hairline images

d Distance from mirror to frosted scale

w $\frac{1}{2}$ the distance between flats

α The angle between the x-axis and the exterior corner of the shaft

C Boundary curve for the cross section

r Radius of shaft

b Width of flat

SUMMARY

This thesis describes and reports the results of an experimental determination of the maximum shearing stress and twisting moment of circular shafts with diametrically opposite flat sides. Five AL-61 Aluminum alloy specimens were tested, one fully round shaft and the remaining four with progressively larger flats. Strains were measured with resistance wire strain gages. Angles of twist were determined by optical means.

An electrical analog experiment was conducted to determine independent results for one of the configurations.

The experimental results obtained by both techniques compared very favorably with mathematical solutions obtained by previous investigators.

CHAPTER I

AN INTRODUCTION TO THE PROBLEM

1. Statement of the problem.

This thesis is a report of an experimental determination of the torsional rigidity and maximum torsional stress occurring in a solid round bar having diametrically opposite flat sides.

2. State of stress for a solid round shaft with diametrically opposite parallel flats.

The state of stress can best be visualized by reference to the membrane analogy for the torsion problem [1]. Considering the deflected surface of the membrane conclusions can be made as to the stress distribution. The shear stress in any direction is proportional to the slope of the surface perpendicular to that direction. It varies from a maximum tangent to the contours to zero perpendicular to the contours. Thus the maximum shear stress acts at points where the contour lines are closest to each other. With this in view reference to Fig. 1, which is a cross section of the shaft, leads one to conclude that the maximum stress will be at the center of the flat sides and zero at the center of the cross section and at the four corners.

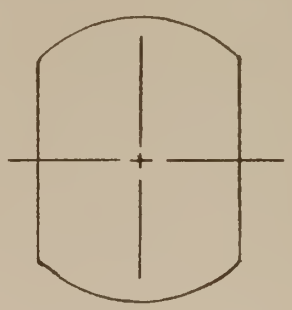

Fig. 1. Cross section of the shaft.

3. Previous solutions to the problem.

H. Ōkubo [2] obtained an approximate solution for maximum shearing

stress employing a variation of the technique given by Shepherd [3]. Ōkubo obtained an approximate solution in the form of elementary functions which satisfied the differential equation but only approximately satisfies the boundary conditions. W. J. Carter and J. B. Oliphint [4] obtained solutions for torsional rigidity and maximum shear stress by numerical relaxation. For very small flats Carter and Oliphint made use of a hydrodynamic analogy to obtain the maximum stress. The above authors carried out the computations for several configurations, but no experimental results were presented. A search of the available literature by the writer disclosed no further work on the problem.

4. Electrical Analogy

The problem considered is that of twisting a prismatical bar with couples applied at the end cross sections (St.-Venant torsion [5]). It is assumed that the bar is homogeneous, isotropic and obeys Hooke's law.

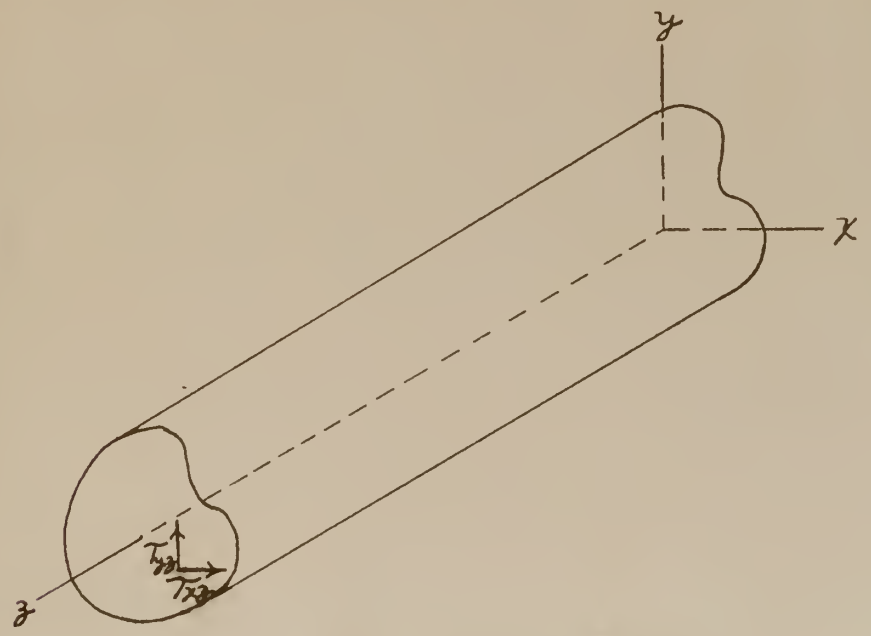

Fig. 2. Bar in Torsion.

St.-Venant showed that the only stress components different from

zero are T_{xz} and T_{yz} (Fig. 2) and that they are functions of x and y only. L. Prandtl [6] introduced the stress function $\phi = \phi(x, y)$ defined by

$$T_{xz} = \frac{\partial \phi}{\partial y} \quad , \quad T_{yz} = -\frac{\partial \phi}{\partial x} \tag{1}$$

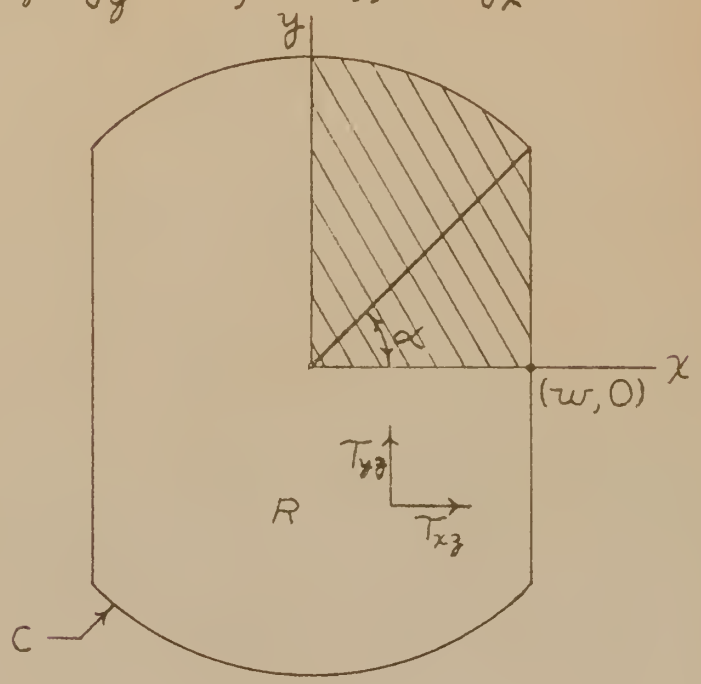

Fig. 3. Cross Section of the Shaft.

The stress function satisfies the partial differential equation

$$\nabla^2 \phi = \frac{\partial^2 \phi}{\partial x^2} + \frac{\partial^2 \phi}{\partial y^2} = -2G\theta \quad \text{in } R \, , \tag{2}$$

and the boundary condition

$$\phi = 0 \quad \text{on C.} \tag{3}$$

G is the shear modulus for the material and θ is the angle of twist per unit length. R is the region of the cross-section of the shaft and C is

its boundary curve (see Fig. 3.) The twisting moment is found by

$$M_t = 2\iint_R \phi \, dx \, dy \tag{4}$$

To transform the problem, assume the stress function has the form

$$\phi = \phi' - \frac{G\theta}{2}(x^2 + y^2) \tag{5}$$

in the region R of Fig. 3 and is equal to zero on the boundary C. Putting this in Eq. (2) gives

$$\nabla^2 \phi' = 0 \tag{6}$$

which is Laplace's equation to be satisfied in R. The boundary condition now reduces to

$$\phi' = \frac{G\theta}{2}(x^2 + y^2) \qquad \text{on C.} \tag{7}$$

Thus the torsional problem reduces to obtaining a solution of Laplace's equation over the cross section and satisfying the boundary condition Eq. (7).

There are many techniques available for obtaining a solution of Laplace's equation. The author chose to use a General Electric Analog Field Plotter with Teledeltos uniform conducting paper because of its simplicity, ease of use and the availability of components. The experimental assembly used is shown in Fig. 4.

Fig. 4. Analog Experimental Assembly.

$$\phi' = K(V) \tag{8}$$

where K is a constant of proportionality and V is the potential. Then by Eq. (7) the potential varies parabolically along the flat side and is constant along the arc. The equipotential lines are lines of constant ϕ'. From the equipotential lines and K, the ϕ' contours can be obtained for the region. Knowing ϕ' enables one to obtain the ϕ contours by means of Eq. (5).

Eqs. (1) now become, by substitution of Eqs. (5) and (8),

$$\tau_{xz} = K\frac{\partial V}{\partial x} - G\theta y \;, \qquad \tau_{yz} = -K\frac{\partial V}{\partial y} + G\theta x \tag{1a}$$

where $\frac{\partial V}{\partial x}$ and $\frac{\partial V}{\partial y}$ are the components of the potential gradient as obtained from the equipotential lines. Eq. (4) now becomes

$$M_t = 2K\iint_R V\,dx\,dy - G\theta\iint_R (x^2+y^2)\,dx\,dy \tag{4a}$$

The first integral may be evaluated using the equipotential plot and the second analytically. Thus the complete state of stress and the torsional moment may be obtained from the electrical analogy.

CHAPTER II

MATERIAL AND TESTING TECHNIQUE EMPLOYED

5. Specimen material and dimensions.

Aluminum alloy AL - 61 was chosen for specimen material because of its low shear modulus and ease of machining. A low shear modulus was desirable in order to produce relatively large strains and angles of twist of the specimen for a given torque, both of which tended to reduce the relative error of the results. A three and one-quarter inch diameter shaft was chosen. From Fig. 5 it can be seen that the stress pattern must change in going from the small chuck diameter to the relatively larger section, this necessitated having a long specimen in order that the ends of the ten inch gage length be approximately three diameters from the section change. By applying Saint-Venant's principle the stress condition in the gage length could be considered as uniform.

6. Method of machining specimens.

The specimens were machined in accordance with Fig. 5 and Table 1.

TABLE 1

SPECIMEN DIMENSIONS

α	r	w	b
0°	1.627 in.	3.255 in.	0
11.0°	1.576 in.	1.545 in.	0.602 in.
25.0°	1.576 in.	1.428 in.	1.331 in.
46.0°	1.576 in.	1.095 in.	2.265 in.
65.7°	1.576 in.	0.648 in.	1.436 in.

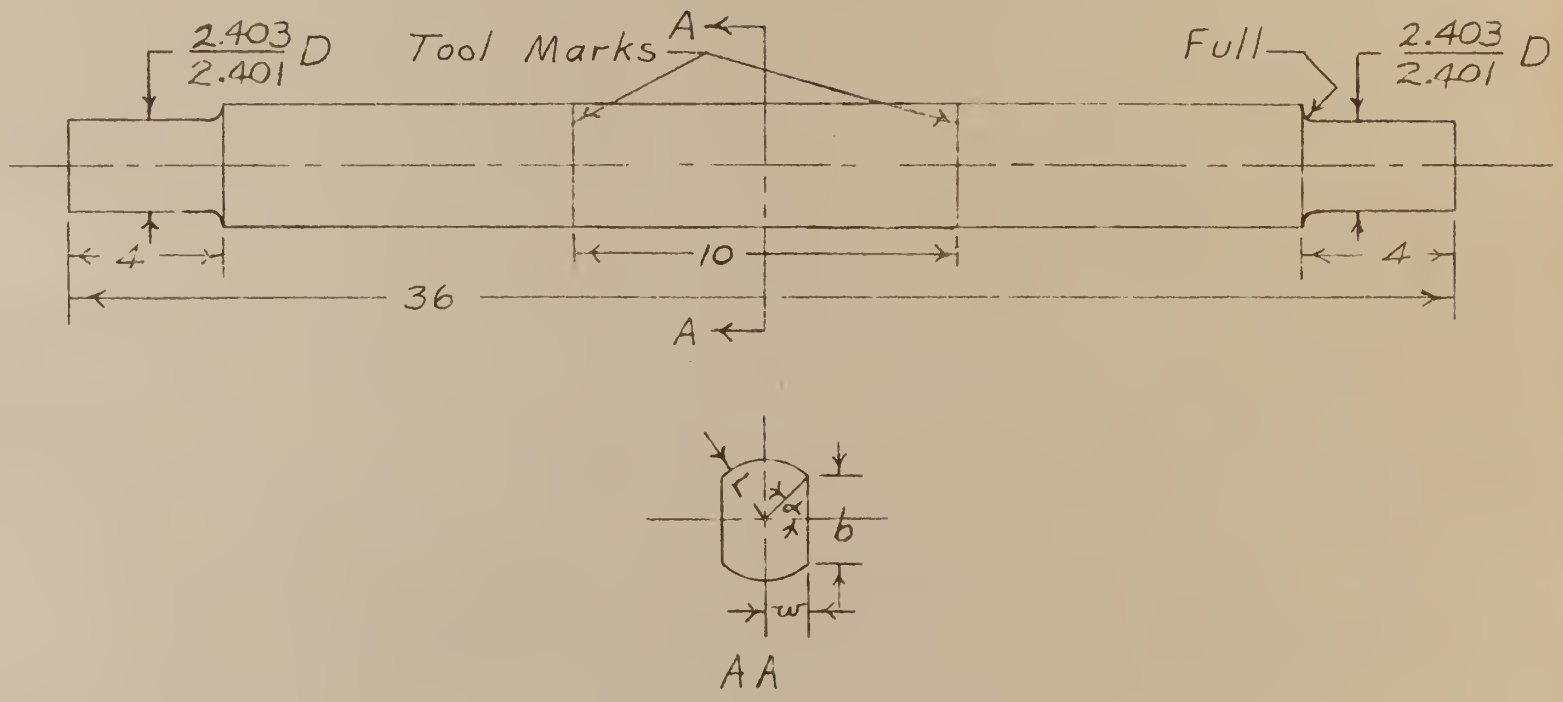

Fig. 5. Specimen details.

The specimens were first machined round and then the flats milled.

All the specimens were checked for axial location and parallelism of the flats and were found to be within one thousandth of an inch which was considered satisfactory.

7. Strain gage selection and application.

The selection of the proper strain gage was an important consideration as it was to be used in the determination of the maximum stress on the flats. The strain varied from zero at the corners to a maximum at the center of the flats, this dictated the selection of a gage as small as practicable. The principal strain directions are at an angle of 45° to the axis of the bar for torsion so a single element gage was chosen. Due to the 45° orientation, the width of the gage element was equally as important a consideration as the length. Two gages were used, one on each flat oriented so as to be ninety degrees to each other, this enabled the separation of unwanted bending strains introduced during testing. Baldwin SR - 4 strain gages were used.

A-19 gages with a one-sixteenth inch by one-sixteenth inch gage element were initially chosen. The use of these gages was abandoned since consistent results could not be obtained when they were tested on the fully round specimen ($\alpha = 0$). Table 2 gives the results obtained from an A-19 gage.

TABLE 2

A-19 STRAIN GAGE RESULTS

Date	Total Drying Time At Room Temperature	Total Drying Time At 160°-170° F	Apparent Strains
4 March	72 hours		0.0123 $\mu \frac{in/in}{in\text{-}lb.}$
6 March	120 hours		0.0134 $\mu \frac{in/in}{in\text{-}lb.}$
12 March	264 hours	20 hours	0.0150 $\mu \frac{in/in}{in\text{-}lb}$
18 March	408 hours	62 hours	0.0154 $\mu \frac{in/in}{in\text{-}lb}$

Two separate A-19 gages were tried but the same phenomenon persisted. Fig. 6 is a typical curve obtained from an A-19 gage, the relaxation on unloading was prevalent on all runs. In view of this, A-7 gages were substituted and they gave consistent results. The A-7 gages have a one-fourth inch gage length and three thirty-seconds inch width. Two AX-5 gages were installed on the fully round specimen for preliminary testing and calibration of the single element gages. All gages were installed and dried using the technique recommended by the manufacturer.

Fig. 6. Strain vs Torque
for
A-19 Strain Gage
12 March 1954

8. Angle of twist measurement.

The maximum angle of twist was less than $\frac{1}{2}$ of 1 degree so an optical means was chosen to measure angles of twist. The schematic diagram for the optical arrangement used at each end of the 10 inch gage length is shown in Fig. 7.

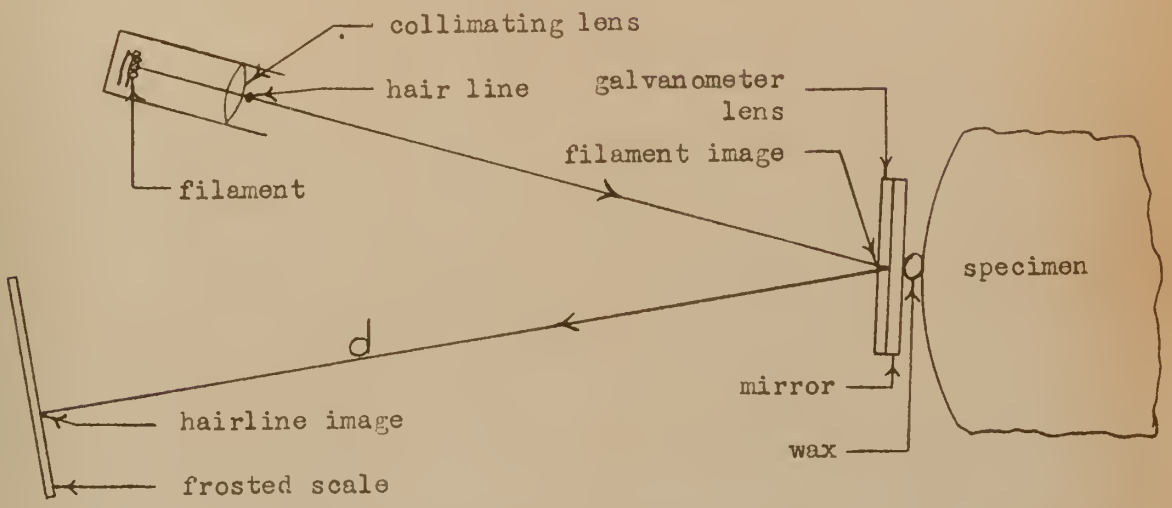

Fig. 7. Schematic diagram for optical system used for angle of twist measurement.

The essential elements are a hairline illuminated by a light source so arranged that the rays from the hairline are reflected by a mirror mounted on the specimen and focused by a galvanometer lens, on a frosted scale. The actual equipment used can be seen in Fig. 8. The hairline images from both the light sources were focused on one frosted scale. Thus differences in the positions of the images on the frosted scale was a measure of the angle of twist in the gage length. Since small angles were involved, the sine, tangent and angle in radians were considered equal. The formula for the angle of twist for a given load is,

$\rho = \frac{\Delta h}{2d}$ where Δh is the change in distance between the hairline images and d is the mirror-to-scale distance. The angle of twist per

unit length for a given load is $\theta = \frac{\varphi}{10}$ where 10 inches is the gage length.

9. Strain gage tests.

The equipment as used is shown in Fig. 8. The specimens were loaded in a standard Tinius - Olsen Torsion Tester on the 0 to 30,000 in-lb range except for the thin specimen ($\alpha = 65.7^{\circ}$) when the 0 to 12,000 in-lb range was used. Two AX - 5 strain gages mounted on the fully round specimen at physical locations ninety degrees apart were used to determine the best method of putting specimens in the machine without introducing extraneous loadings. If the rotating head of the machine was at or near zero degrees and the chucks were tightened slowly and alternately the machine applied essentially pure torsion. Two runs were made on each specimen, one with each gage in the up position. A Baldwin Southwark Type K Strain Indicator was used with a Baldwin S R - 4 12 Channel Switching and Balancing Unit to measure all strains. The temperature compensating gages were mounted on a separate piece of the same material. The specimens were loaded and unloaded in equal increments. After each increment of load had been applied the strains, hairline image positions on the frosted scale and load were recorded. Strains were read to the nearest μ in/in, load to the nearest 10 inch-lb. and hairline image position to the nearest tenth of a millimeter.

10. Analog Experiment

The equipment used for the analog experiment is shown in Fig. 4. It is a General Electric Analog Field Plotter. The experiment was carried out only for $\alpha = 45^{\circ}$, $w = 30$ in . As can be seen in Fig. 3, α is the angle between the x axis and the exterior corner of the

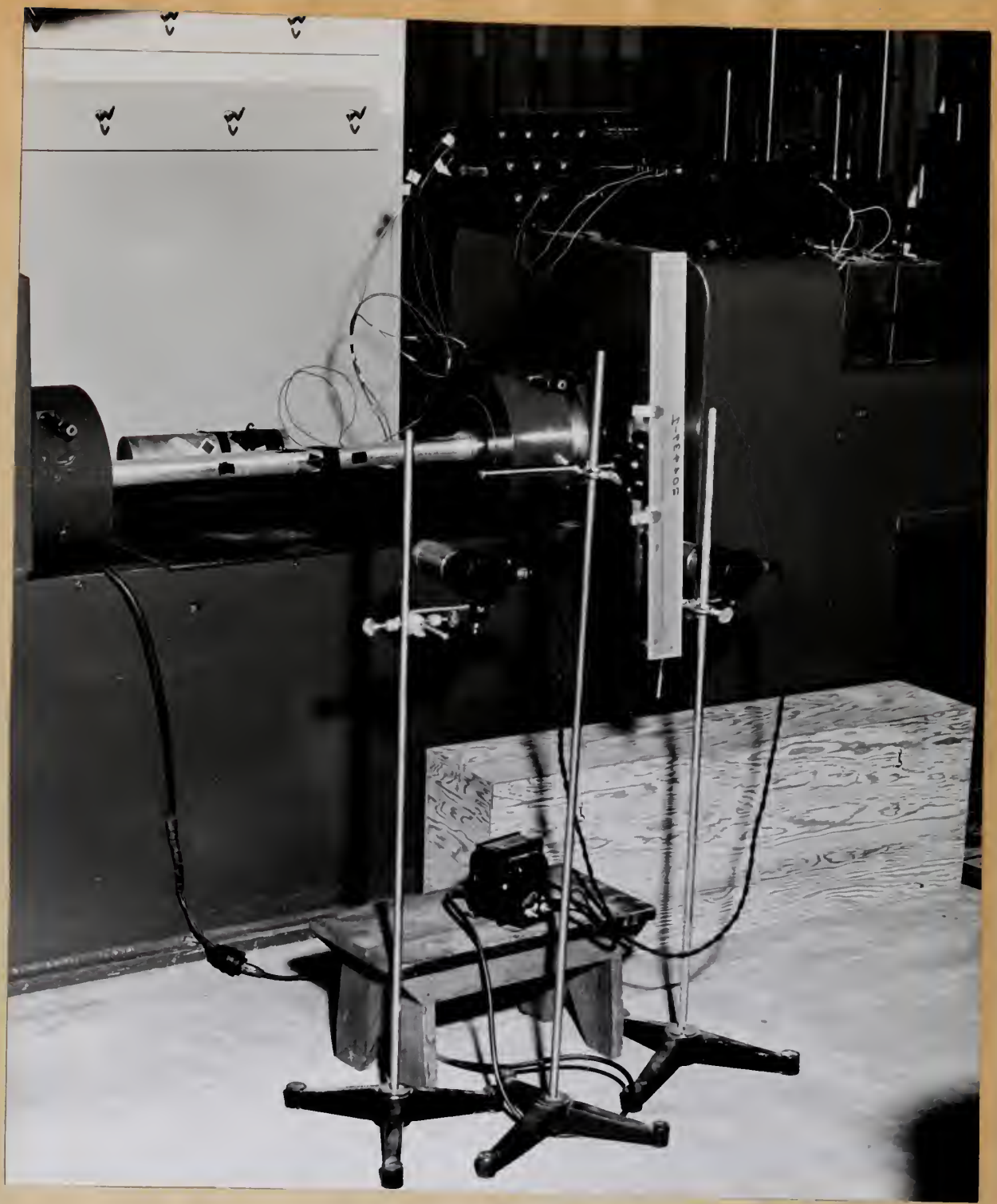

Fig. 8. Experimental Equipment Set Up

shaft, and w is $\frac{1}{2}$ the distance between flats. Due to the double symmetry of the cross section the conducting sheet represented only $\frac{1}{4}$ of the cross section as shown by the shaded area in Fig. 3. The large dimensions were chosen to increase the accuracy of the results.

The null method of determining potentials made it convenient to record experimental potentials P on an arbitrary scale. Accordingly, the potential at the center of the flat (w ,0) was taken as 0 and that on the curved portion of the boundary was taken as 1. As is shown later, the potential V of Eq. 8 is related to the experimental potential P by the equation V = 1+P.

The parabolic potential distribution along the boundary $x = w$ was approximated by a series of linear potential drops. Fig. 9 shows the desired parabolic distribution and how it was approximated by a series of linear drops. There was no net gain or loss of area under the curve. Small increments were taken at the center of the flat in order to have the smallest deviation from the desired distribution, and keep errors in potential gradient to insignificant magnitudes in this region. Table 3 gives the potentials maintained at the chosen locations along the boundary.

TABLE 3

POTENTIALS MAINTAINED ALONG BOUNDARY

Y (in.)	P
0	0
$\frac{1}{2}$	0
2	0.0039
4	0.0162
7	0.0498
12	0.1554
17	0.3165
22	0.5332
27	0.8054
30	1.000

The experimental potentials measured along the boundary are plotted in Fig. 9. To establish the above potential points along the boundary with linear drops between points, 0.004 inch diameter Advance wire with lead wires soldered to it at the selected locations was clamped onto the boundary of the paper by the clamping arrangement shown in Fig. 4. The lead wires were connected to a slide wire potentiometer which was across the output voltage of the rectifier unit. The actual boundary potentials were established 0.15 inch in from the wire by varying the positions of the lead wires on the slide potentiometer. It was found that if the correct potential distribution was set along the boundary wire the actual potential distribution in the adjacent paper was significantly different. The constant potential along the curved portion of the boundary

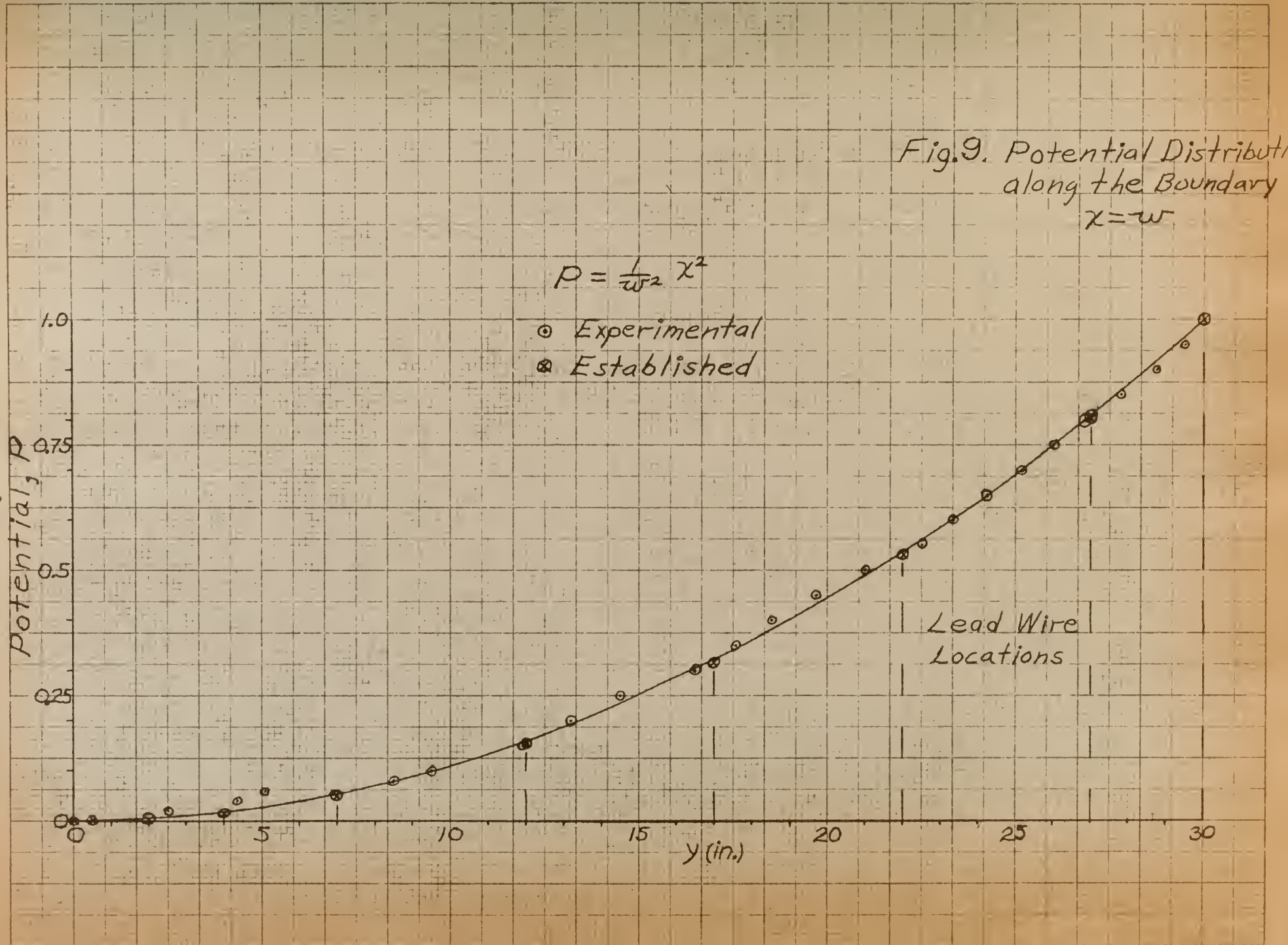
Fig.9. Potential Distribution along the Boundary $x = w$
$P = \frac{1}{w^2} x^2$
Experimental
Established
Potential, P
1.0
0.75
0.5
0.25
0
0
5
10
15
20
25
30
y (in.)
Lead Wire Locations

was maintained by use of silver paint backed by a copper strip. The equipotentials were plotted using standard null technique.

CHAPTER III

REDUCTION OF DATA

11. Strain gage calibration.

The AX-5 strain gages on the fully round specimen were used to calibrate the single element A-7 gages. This was necessary because the gage factor given by the manufacturer gives correct results for uniaxial stress in the direction of the gage length. The gage factor for this strain condition was found from

$$\epsilon = \left[\frac{\text{A-7 Manufacturer's gage factor}}{\text{A-7 gage factor for this strain condition}}\right] e$$

where ϵ is the strain in the direction of the A-7 gage as obtained from the AX-5 gages and e is the apparent strain obtained by the A-7 gage when the manufacturer's gage factor was set on the indicator. The manufacturer's gage factor was 1.95 and the apparent gage factor for this strain condition was found to be 1.97. It is noted that this result implies a negative transverse sensitivity for the A-7 gage. This is in agreement with transverse sensitivities reported by Baumberger and Hines [7].

12. Electrical Analogy

The computation of the maximum stress at the center of the flat and the computations for torsional moment were carried out as discussed in section 4. By Eqs. (8) and (5), $\phi' = K(V) = \frac{G\theta}{2}(x^2 + y^2)$. At $(w, 0)$, $KV_1 = \frac{G\theta}{2}(w^2)$ and at (w, w), $KV_2 = G\theta w^2$. Taking the applied potential difference as unity, $V_2 - V_1 = 1$. Then $K = \frac{G\theta w^2}{2}$, $V_2 = 2$, $V_1 = 1$. The potential at any point on the surface is, $V = V_1 + P = 1 + P$ where P is the experimental potential. Fig. 10 shows the equipotentials over a quarter of the cross section. At $(w, 0)$ $\tau_{xz} = 0$ and

$$\tau_{yz} = -\frac{\partial \phi'}{\partial x} + G\theta x = -\frac{G\theta w^2}{2}\left.\frac{\partial P}{\partial x}\right]_{(w,0)} + G\theta w$$

$\left.\frac{\partial P}{\partial x}\right]_{(w,0)}$ is obtained from Fig. 11. Eq. (4a) now becomes

$$M_t = G\theta w^2 \iint_R (1 + P)\, dx\, dy - G\theta \iint_R (x^2 + y^2)\, dx\, dy \qquad (4a)$$

Simpson's one-third rule for approximate integration was used to obtain the volume under the potential surface for evaluating the first integral. The value of the last integral was obtained analytically.

Fig. 10. Equipotential Traces of Electrical Analog.

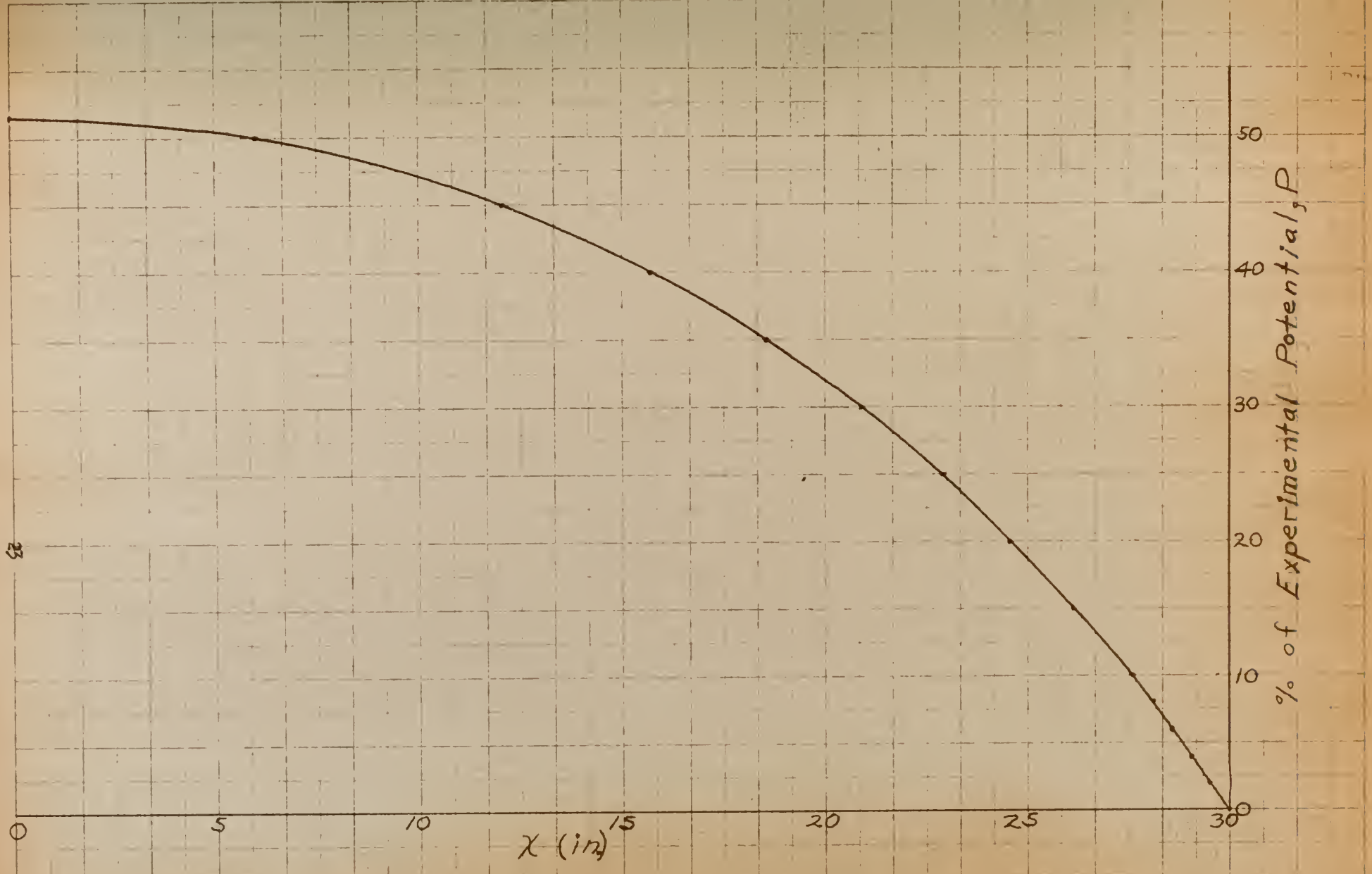

Fig. 11. Experimental Potential vs Distance Along x-Axis

CHAPTER IV

RESULTS AND DISCUSSION

13. The results.

Numerical results obtained from tests are given in Table 4. The values for $\alpha = 45^\circ$ were obtained by the electrical analogy.

TABLE 4

VALUES OF MAXIMUM SHEAR STRESS

AND TWISTING MOMENT

α	T_{max}	M_t
0°	$1.00\, G\theta w$	$1.58\, G\theta r^4$
11°	$1.13\, G\theta w$	$1.57\, G\theta r^4$
25°	$1.31\, G\theta w$	$1.44\, G\theta r^4$
45°	$1.66\, G\theta w$	$0.964\, G\theta r^4$
46°	$1.58\, G\theta w$	$0.923\, G\theta r^4$
65.7°	$1.87\, G\theta w$	$0.257\, G\theta r^4$

r is the radius of the shaft.

14. Comparison with previous solutions.

Fig. 12 gives a comparison of the present results with those of previous investigators. Carter and Oliphint stated that they believed their results were accurate to within 2 or 3 per cent. Ōkubo gave no figures for accuracy of his results.

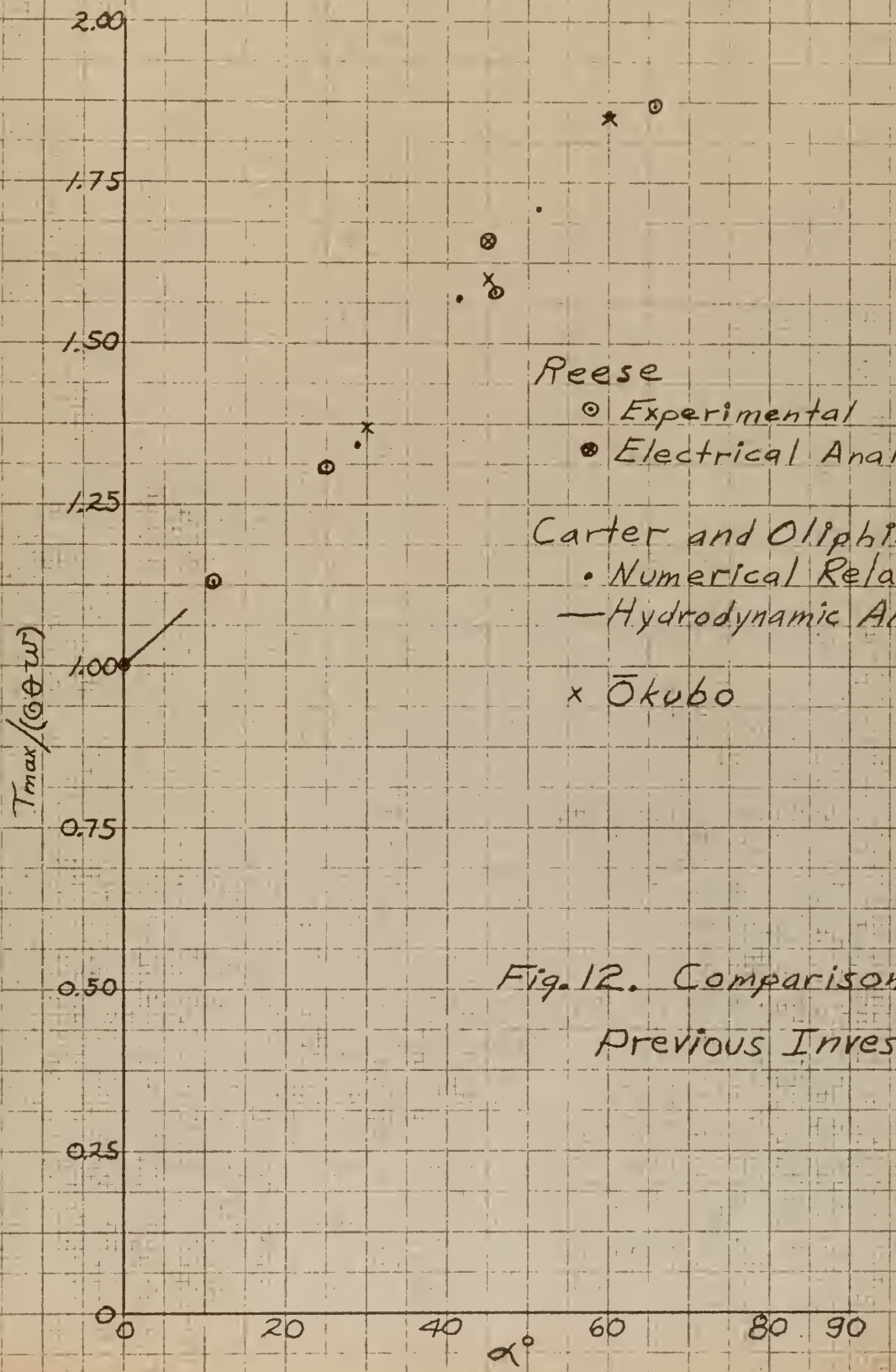

Fig. 12. Comparison with Previous Investigations.

15. Sources of error.

The strain vs torque relationship obtained with the AX-5 strain gages on the fully round specimen was linear within reading accuracy. The extraneous bending stresses introduced by the torsion machine were found to be less than 1% of the torsional stress. Results were corrected for bending stresses by averaging readings of gages on opposite flats. The orientation of the strain gages is believed to have been within 1° of the desired 45° orientation. Location of the mirrors on the 10 inch gage length was within ± 1/16 inch. The strain gage elements covered a finite area on the flats of the shaft and the stress varies from zero at the exterior corners to a maximum at the center of the flat. Thus the strains indicated by the gages were not the maximum but some sort of average over the gage element. This error is believed to be small.

The manufacturer of the Teledeltos paper states that it has anisotropic variations of ±3 to ±8% maximum deviations from a mean value of resistance. The rated linearity of the potentiometer used to establish the equipotentials was ±½%. No correction was made for the boundary potential being established 0.15 inch in the interior.

The optical system used for measuring angles of twist gave reading accuracies of 1% of the total angle of twist. The obtaining of greater accuracy would have greatly complicated the optical system.

The overall results are believed to be accurate to within 4%.

CHAPTER V

CONCLUSION

The experimental results checked closely with the previous mathematical solutions to the problem. Although the results obtained by the electrical analogy were reliable, the work involved was many times that of the direct experimentation for the same specimen configuration.

BIBLIOGRAPHY

1. Timoshenko, S. and J. N. Goodier. Theory of Elasticity. New York, McGraw-Hill, 1951

2. Ōkubo, H. Torsion of a Circular Shaft with a Number of Longitudinal Notches. Journal of Applied Mechanics. Vol. 17, 1950, Pg. 359.

3. Shepherd, W. M. The Torsion and Flexure of Shafting with Keyways of Cracks. Proceedings of the Royal Society of London, Series A, Vol. 138, 1932, pg. 607 - 634.

4. Carter, W. J. and Oliphint, J. B. Torsion of a Circular Shaft with Diametrically Opposite Flat Sides. Journal of Applied Mechanics, September, 1952.

5. Todhunter, I. and Pearson, K. History of the Theory of Elasticity, Vol. 2.

6. Prandtl, L. Physik. Z , Vol. 4, 1903.

7. Baumberger, R. and Hines, F. Practical Reduction Formulas for use on Bonded Wire Strain Gages in Two-Dimensional Stress Fields. Experimental Stress Analysis, Vol. II, No. 1.

Thesis
R275

Reese
Torsion of a circular shaft with diametrically opposite flat sides.

25271

Thesis
R275

Reese
Torsion of a circular shaft with diametrically opposite flat sides.